**ARTICLE TYPE**

# New Low-Voltage Plateau of Na$_3$V$_2$(PO$_4$)$_3$ Anode for Na-Ion Batteries†

**Zelang Jian,**[a,‡] **Yang Sun,**[b,‡] **Yong-Sheng Hu**[b,*] **and Xiulei Ji**[a,*]

5 **A low-voltage plateau at ~ 0.3 V is discovered during the deep sodiation of Na$_3$V$_2$(PO$_4$)$_3$ by combined computational and experimental studies. This new low-voltage plateau doubles the sodiation capacity of Na$_3$V$_2$(PO$_4$)$_3$, thus turning it a promising anode for Na-ion batteries.**

10 Renewable energy sources, such as wind and solar energy, are promising to cope with the global energy shortage. However, their intermittent nature demands cost-effective energy storage solutions. Among electrochemical energy storage technologies,[1] Li-ion batteries (LIBs) exhibit superior performance, but their
15 large-scale applications are limited by the rarity of lithium resource. Sodium, as the second smallest alkali element, shows similar electrochemical properties as lithium.[1] Recently, Na-ion batteries (NIBs) have attracted much attention because of the abundance and wide distribution of sodium resource. Numerous
20 materials have been investigated as electrodes for NIBs, such as carbon[2], alloys[3], metal oxides[4], polyanion-structure materials[5], layered oxides[6], tunnel-structured oxides[7] and organic materials[8]. Among them, polyanion-structure materials[5], such as transition metal fluorophosphates[9] and phosphates[10], possess stable host
25 structures for topotatic intercalational reactions, which extends the successes of the same classes of materials in LIBs.[11]

Na$_3$V$_2$(PO$_4$)$_3$ crystallizes in the rhombohedral NASICON (Na super ionic conductor) structure. Its well-known three-dimensional (3D) network structure facilitates fast ionic diffusion.
30 Jian *et al.* have shown that two Na ions can be reversibly extracted from Na$_3$V$_2$(PO$_4$)$_3$, exhibiting a desodiation voltage plateau at 3.4 V, which makes this compound a promising cathode material for NIBs.[12] Note that all potentials in this paper are *vs.* Na$^+$/Na. The carbon-coated Na$_3$V$_2$(PO$_4$)$_3$ nearly delivers its
35 theoretical capacity of 117 mAh/g, excellent capacity retention over cycling and high rate capability.[13] On the other hand, Na$_3$V$_2$(PO$_4$)$_3$ is able to function as a NIB anode as well, with a sodiation voltage plateau of 1.6 V.[12] The plateau corresponds to the insertion of one Na ion to form Na$_4$V$_2$(PO$_4$)$_3$, resulting in a
40 capacity half that of its cathode reaction. In contrast, its lithium counterpart, rhombohedral Li$_3$V$_2$(PO$_4$)$_3$, can be lithiated with two Li ions, thus giving rise to a capacity of ~ 120 mAh/g as a LIB anode.[14] Therefore, we are interested to reveal whether Na$_3$V$_2$(PO$_4$)$_3$ can be sodiated with two Na ions?

45 In this work, we conduct a combined computational and experimental investigation on the sodiation properties of Na$_3$V$_2$(PO$_4$)$_3$ as a NIB anode. Both theoretical calculations and experiments indicate that two Na ions, instead of one, can be inserted into the structure of Na$_3$V$_2$(PO$_4$)$_3$ in two sequential
50 distinct plateaus at about 1.6 V and 0.3 V, respectively. The two Na ions are inserted into unoccupied 18e and 6a sites, respectively. To the best of our knowledge, the plateau at 0.3 V is discovered for the first time. Moreover, the carbon-coated Na$_3$V$_2$(PO$_4$)$_3$ anode delivers great cycling and rate performance
55 upon deep sodiation.

Na$_3$V$_2$(PO$_4$)$_3$ and Li$_3$V$_2$(PO$_4$)$_3$ have an analogous skeleton structure of V$_2$(PO$_4$)$_3$, which consists of corner-shared VO$_6$ octahedra and PO$_4$ tetrahedra. However, the occupancies of Na ions and Li ions are different. For Na$_3$V$_2$(PO$_4$)$_3$, two Na ions
60 occupy 18e sites and one Na ion occupies the 6b site, whereas all three Li ions occupy the 18f sites of Li$_3$V$_2$(PO$_4$)$_3$. During lithiation, Li$_3$V$_2$(PO$_4$)$_3$ can take in two Li ions that occupy the 3a (0.5 Li), 3b (0.5 Li), and 6c (1 Li) sites, respectively.[14] On the other hand, during sodiation of Na$_3$V$_2$(PO$_4$)$_3$, it is known that one
65 Na ion can be inserted to the last empty 18e site, resulting in a voltage plateau at 1.6 V. Note that the 6a site is also empty, which may accommodate one more Na ion; however, to date, the second Na ion insertion into the Na$_3$V$_2$(PO$_4$)$_3$ electrode has not been reported.

70 To understand the Na-ion storage by Na$_3$V$_2$(PO$_4$)$_3$ at low voltages, we first perform first-principles calculations based on density functional theory (DFT). According to the method proposed by Ceder *et al.*[15], the average voltage could be obtained by calculating the supercell energy of Na$_x$V$_2$(PO$_4$)$_3$ with different
75 *x* values, the number of Na ions per formula unit. Based on the crystal structures of NaV$_2$(PO$_4$)$_3$, Na$_3$V$_2$(PO$_4$)$_3$[16] and Na$_4$V$_2$(PO$_4$)$_3$, (Figure S1, Figure 1b), our calculations show voltage plateaus at 3.32 V for the desodiation of Na$_3$V$_2$(PO$_4$)$_3$ to NaV$_2$(PO$_4$)$_3$ and 1.95 V for sodiation of Na$_3$V$_2$(PO$_4$)$_3$ to Na$_4$V$_2$(PO$_4$)$_3$, respectively,
80 in good agreement with previous computational and experimental results.[12, 16b] In this study, calculations predict a low plateau located at 0.33 V, corresponding to further sodiation to Na$_5$V$_2$(PO$_4$)$_3$ (Figure 1). Figure 1b illustrates the unit cells of Na$_4$V$_2$(PO$_4$)$_3$ and Na$_5$V$_2$(PO$_4$)$_3$, where Na ion coordination
85 numbers (CN) at the 6b and 6a sites are the same of 6, compared to 8 at the 18e sites.[16a] Compared to 18e sites, sodiation to the 6a site is energetically unfavourable due to the greater Coulombic repulsion, thus leading to a low voltage plateau.

We conduct electrochemical experiments to verify above
90 calculation results. Carbon-coated Na$_3$V$_2$(PO$_4$)$_3$ electrode is synthesized by previously reported methods[14], where carbon content is 5 wt.%. X-ray differaction (XRD) pattern confirms the phase-pure of Na$_3$V$_2$(PO$_4$)$_3$ with lattice parameters of *a* = 8.726 Å,

$c$ = 21.825 Å, consistent with the previous results (Figure 2).[16a] The Rietveld refinement results are summarized in Table S1. Two Na ions occupy two of three 18e sites, one takes the 6b site, and the 6a site is empty, indicating that two more Na ions can be accommodated by this structure.
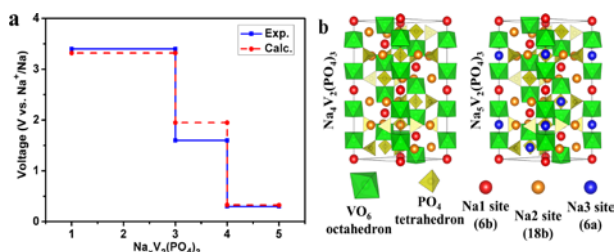


**Figure 1** a. Calculated sodiation voltage profile (red dotted line) of $Na_3V_2(PO_4)_3$ in comparison to the experimentally determined voltage profile (blue solid line). b. Schematic illustration of the unit cells of $Na_4V_2(PO_4)_3$ (left) and $Na_5V_2(PO_4)_3$ (right).

$Na_3V_2(PO_4)_3$/C electrodes are tested with sodium metal as the counter/reference electrode and 1 M $NaPF_6$ in ethylene carbonate–dimethyl carbonate (EC–DMC, 1:1 v/v) as the electrolyte. Cyclic voltammetry (CV) profiles are collected at a scan rate of 0.05 mV/s in a voltage range of 0-3 V. Figure 3a displays two sets of primary redox peaks around ~1.6 V and ~ 0.3 V, respectively, and one set of minor redox peaks near 0 V. During sodiation, the 18e sites become completely filled, resulting the peak near 1.6 V.[16a] The second redox peak at ~ 0.3 V is consistent with our computational prediction, where the second Na ion occupies the 6a site. Note that the minor redox peaks close to 0 V is most likely due to the sodiation/desodiation of the carbon coating layer composed of hard carbon pyrolyzed from glucose and the conducting carbon additive in the electrode. The typical sodiation/desodiation profiles of hard carbon comprise a slope and a plateau at very low potentials, as shown in Figure S2. In the 1st CV cycle, there is a cathodic peak at ~ 0.5 V, which is attributed to the formation of solid electrolyte interphase (SEI). Note that no corresponding anodic peak is observed. Subsequent CV curves overlap well, indicating reversible redox reactions.
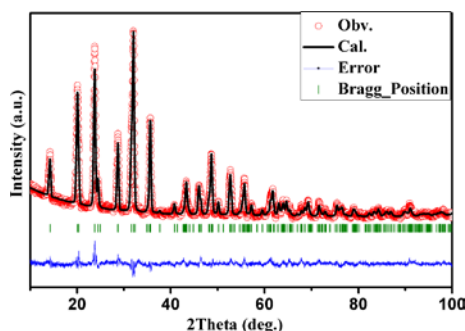


**Figure 2**. Rietveld refinement of $Na_3V_2(PO_4)_3$/C XRD. Red circles represent the observed intensities. Black solid line shows calculated pattern. Blue curve tells the difference between the observed and calculated intensities. Green vertical bars indicate Bragg reflections of $Na_3V_2(PO_4)_3$.
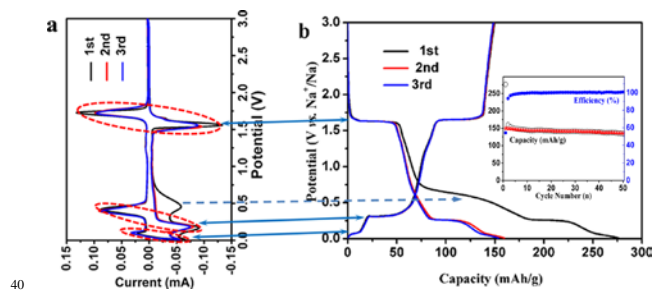


**Figure 3**. a. CV curves of the $Na_3V_2(PO_4)_3$/C in 0-3 V. b. Sodiation/desodiation profiles of $Na_3V_2(PO_4)_3$/C at a current rate of 0.1 C. Inset: the corresponding cycling performance.

The sodation/desodiation profiles at a current density of 11.7 mA/g (0.1 C, C-rate is defined as 117 mAh/g) are shown in Figure 3b. There are three flat plateaus, located at 1.6 V, 0.3 V and 0.05V, respectively, consistent with the redox peaks in the CV curves. The long slope in the initial sodiation curve is caused by the SEI formation, corresponding to the cathodic peak at 0.5 V in the CV curve. The initial sodiation capacity is 277 mAh/g and the reversible desodiation capacity is 149 mAh/g. The latter is higher than the theoretical capacity for insertion of two Na ions. The exceeding capacity is attributed to the capacity carbon coating layer (~ 15 mAh/g) and carbon additives (~ 20 mAh/g) contribute.

The typical sodiation curve (the 2nd cycle) can be roughly divided into four sections (see Figure S3). Section I, a plateau region, is associated with the insertion of the first Na ion that occupies the third 18e site, where the corresponding capacity is about ~59 mAh/g. Section III corresponds to the insertion of the second Na ion that occupies the 6a site, where the capacity is ~ 54 mAh/g. These results suggest that two Na ions are inserted into the $Na_3V_2(PO_4)_3$, in good agreement with the calculations. Section II is probably attributed to the carbon coating layer and the carbon additive (sloping region of carbon sodiation). Section IV may be caused by carbon as well from the plateau region of carbon sodiation.
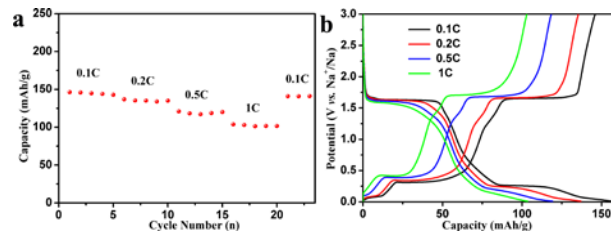


**Figure 4.** a. The rate performance of the $Na_3V_2(PO_4)_3$/C sample at rates of 0.1, 0.2, 0.5 and 1C. b. Typical sodiation/desodiation curves of the $Na_3V_2(PO_4)_3$/C sample at different rates

Figure 3b inset shows the cycling and rate performance of the $Na_3V_2(PO_4)_3$/C electrode. After 50 sodiation/desodiation cycles at 0.1C, the capacity is 136 mAh/g, 91% retention, where the Coulombic efficiency increases to ca. 100% after the initial 5 cycles. We attribute the good cycling performance to the stable NASICON host structure.[12a, 17] Reversible desodiation capacities of 147, 136, 118, and 103 mAh/g are obtained at rates of 0.1, 0.2, 0.5, and 1C, respectively, as shown in Figure 4a. At 1C, the

desodiation curve still shows the well maintained plateaus (Figure 4b), which indicates the high-rate behaviour of the two-phase reactions of $Na_3V_2(PO_4)_3$. Considering the large particle size, ~1-5 μm (Figure S4), the rate performance of $Na_3V_2(PO_4)_3$/C is very promising, which should be ascribed to the NASICON structure and its highly covalent 3D framework with large interstitial spaces for Na ion diffusion.[18]

In conclusion, a new plateau at ~0.3 V is revealed for the first time for $Na_3V_2(PO_4)_3$ as an anode via combined computational and experimental studies. This new plateau corresponds to the insertion of the second Na ion into the 6a site of $Na_3V_2(PO_4)_3$ during deep sodiation. Therefore, altogether five Na ions can be accommodated in the $V_2(PO_4)_3$ host, occupying the 18e (three Na ions), 6a (one Na ion), and 6b (one Na ion) sites, respectively. The new low-voltage plateau doubles the specific capacity of $Na_3V_2(PO_4)_3$/C as an NIBs anode. The $Na_3V_2(PO_4)_3$/C electrode delivers stable cycling performance with 91% capacity retention after 50 cycles at 0.1 C and good rate performance, reaching a capacity of 103 mAh/g at a high rate of 1C. Further investigation on its Na storage and phase transformation mechanisms is ongoing.

## Notes and references

[a] Department of Chemistry, Oregon State University, Corvallis, OR, USA, 97331-4003, United States. E-mail: David.Ji@oregonstate.edu

[b] Key Laboratory for Renewable Energy, Beijing Key Laboratory for New Energy Materials and Devices, Beijing National Laboratory for Condensed Matter Physics, Institute of Physics, Chinese Academy of Sciences, Beijing 100190, China. Email: yshu@aphy.iphy.ac.cn

† Electronic Supplementary Information (ESI) available. See DOI: XXXXXX

‡ Z. Jian and Y. Sun contributed equally to this work.

1 (a) M. D. Slater, D. Kim, E. Lee and C. S. Johnson, *Advanced Functional Materials*, 2013, **23**, 947; (b) H. Pan, Y.-S. Hu and L. Chen, *Energy & Environmental Science*, 2013, **6**, 2338; (c) D. Larcher and J. Tarascon, *Nature Chemistry*, 2014; (d) N. Yabuuchi, K. Kubota, M. Dahbi and S. Komaba, *Chemical reviews*, 2014; (e) S. W. Kim, D. H. Seo, X. Ma, G. Ceder and K. Kang, *Advanced Energy Materials*, 2012, **2**, 710.

2 (a) Y. Li, S. Xu, X. Wu, J. Yu, Y. Wang, Y.-S. Hu, H. Li, L. Chen and X. Huang, *Journal of Materials Chemistry A*, 2015, **3**, 71; (b) W. Luo, C. Bommier, Z. Jian, X. Li, R. G. Carter, S. Vail, Y. Lu, J.-J. Lee and X. Ji, *ACS applied materials & interfaces*, 2015, DOI: 10.1021/am507679x.

3 (a) Y. Liu, N. Zhang, L. Jiao, Z. Tao and J. Chen, *Advanced Functional Materials*, 2014; (b) Y. Zhu, X. Han, Y. Xu, Y. Liu, S. Zheng, K. Xu, L. Hu and C. Wang, *ACS nano*, 2013, **7**, 6378.

4 (a) Y. Sun, L. Zhao, H. Pan, X. Lu, L. Gu, Y.-S. Hu, H. Li, M. Armand, Y. Ikuhara and L. Chen, *Nature Communications*, 2013, **4**, 1870; (b) S. Yuan, X. l. Huang, D. l. Ma, H. g. Wang, F. z. Meng and X. b. Zhang, *Advanced Materials*, 2014, **26**, 2273; (c) Z. Jian, B. Zhao, P. Liu, F. Li, M. Zheng, M. Chen, Y. Shi and H. Zhou, *Chemical Communications*, 2014, **50**, 1215.

5 (a) P. Barpanda, T. Ye, S.-i. Nishimura, S.-C. Chung, Y. Yamada, M. Okubo, H. Zhou and A. Yamada, *Electrochemistry Communications*, 2012, **24**, 116; (b) C. Masquelier and L. Croguennec, *Chemical reviews*, 2013, **113**, 6552.

6 (a) N. Yabuuchi, M. Kajiyama, J. Iwatate, H. Nishikawa, S. Hitomi, R. Okuyama, R. Usui, Y. Yamada and S. Komaba, *Nature materials*, 2012, **11**, 512; (b) M. Guignard, C. Didier, J. Darriet, P. Bordet, E. Elkaïm and C. Delmas, *Nature materials*, 2013, **12**, 74; (c) Y. Wang, X. Yu, S. Xu, J.

Bai, R. Xiao, Y.-S. Hu, H. Li, X.-Q. Yang, L. Chen and X. Huang, *Nature Communications*, 2013, **4**.

7 E. Hosono, T. Saito, J. Hoshino, M. Okubo, Y. Saito, D. Nishio-Hamane, T. Kudo and H. Zhou, *Journal of Power Sources*, 2012, **217**, 43.

8 (a) L. Zhao, J. Zhao, Y. S. Hu, H. Li, Z. Zhou, M. Armand and L. Chen, *Advanced Energy Materials*, 2012, **2**, 962; (b) W. Luo, M. Allen, V. Raju and X. Ji, *Advanced Energy Materials*, 2014, **4**, 1400554.

9 R. Gover, A. Bryan, P. Burns and J. Barker, *Solid State Ionics*, 2006, **177**, 1495.

10 (a) J. Zhao, Z. Jian, J. Ma, F. Wang, Y. S. Hu, W. Chen, L. Chen, H. Liu and S. Dai, *ChemSusChem*, 2012, **5**, 1495; (b) R. Tripathi, S. M. Wood, M. S. Islam and L. F. Nazar, *Energy & Environmental Science*, 2013, **6**, 2257.

11 A. K. Padhi, K. Nanjundaswamy and J. B. d. Goodenough, *Journal of The Electrochemical Society*, 1997, **144**, 1188.

12 (a) Z. Jian, W. Han, X. Lu, H. Yang, Y. S. Hu, J. Zhou, Z. Zhou, J. Li, W. Chen and D. Chen, *Advanced Energy Materials*, 2013, **3**, 156; (b) Z. Jian, L. Zhao, H. Pan, Y.-S. Hu, H. Li, W. Chen and L. Chen, *Electrochemistry Communications*, 2012, **14**, 86.

13 C. Zhu, K. Song, P. A. van Aken, J. Maier and Y. Yu, *Nano letters*, 2014, **14**, 2175.

14 Z. Jian, W. Han, Y. Liang, Y. Lan, Z. Fang, Y.-S. Hu and Y. Yao, *Journal of Materials Chemistry A*, 2014, **2**, 20231.

15 G. Ceder, M. Aydinol and A. Kohan, *Computational materials science*, 1997, **8**, 161.

16 (a) Z. Jian, C. Yuan, W. Han, X. Lu, L. Gu, X. Xi, Y. S. Hu, H. Li, W. Chen and D. Chen, *Advanced Functional Materials*, 2014; (b) S. Y. Lim, H. Kim, R. Shakoor, Y. Jung and J. W. Choi, *Journal of The Electrochemical Society*, 2012, **159**, A1393.

17 C. D. Wessells, S. V. Peddada, R. A. Huggins and Y. Cui, *Nano letters*, 2011, **11**, 5421.

18 (a) C. Delmas, R. Olazcuaga, F. Cherkaoui, R. Brochu and G. Leflem, *Comptes Rendus Hebdomadaires Des Seances De L Academie Des Sciences Serie C*, 1978, **287**, 169; (b) J. Gopalakrishnan and K. K. Rangan, *Chemistry of materials*, 1992, **4**, 745.